65° CONGRESSO ABM INTERNACIONAL
65th ABM INTERNATIONAL CONGRESS
ANAIS PROCEEDINGS
ISSN 1516-392X

EFFECTS OF HYDROGEN PRESSURE AND TEST FREQUENCY ON FATIGUE CRACK GROWTH PROPERTIES OF NI-CR-MO STEEL (JIS-SNCM439)[1]

Arnaud Macadre[2]
Saburo Matsuoka[3]
Yukitaka Murakami[4]
Françoise Barbier[5]
Jader Ferreira Furtado Filho[6]

Abstract
Fatigue crack propagation tests were carried out on Ni-Cr-Mo (JIS-SNCM439) steel in order to investigate the effect of hydrogen pressure and loading frequency on the crack propagation rate. Hydrogen pressure has well affected the crack propagation acceleration rate, being around 86 times faster for a fixed ΔK value of 17.5 MPa.m1/2 and 90 MPa of hydrogen pressure. The impact of frequency was dependent upon the hydrogen pressure employed during the tests. At 90 MPa of hydrogen pressure, as it was expected, lower frequencies have generated faster crack growth rates, but at 0.6 MPa the crack propagation has presented an unusual result as the da/dN was slower for the frequencies bellow 1 Hz, which is contrary to the usual assumption that lower frequencies will conduct to higher crack growth rates due to the hydrogen embrittlement effect. The fracture surfaces of specimens analyzed with SEM have indicated that the number of facets and striation spacing were also affected by hydrogen.
Key words: Hydrogen embrittlement; Fatigue crack propagation; Ni-Cr-Mo steel; JIS-SNCM439.

EFEITOS DA PRESSÃO DO HIDROGÊNIO E DA FREQUÊNCIA NA PROPAGAÇÃO DE TRINCAS DE FADIGA DO AÇO NI-CR-MO (JIS-SNCM439)

Resumo
Testes de propagaçao de trinca foram realizados no aço Ni-Cr-Mo (JIS-SNCM439) à fim de se investigar o effeito da pressão de hidrogênio e da frequência de carregamento na taxa de propagaçao da trinca. O efeito do hidrogênio foi pronunciado, chegando a alcançar uma taxa de aceleraçao em torno de 86 vezes superior à taxa de propagaçao de uma amostra testada ao ar de laboratorio para os ensaios realizados a um valor de ΔK constante igual a 17.5 MPa.m$^{1/2}$ e pressão de H_2 de 90 MPa. O impacto da frequencia foi afetado pela pressao de teste. Sob uma pressao de hidrogênio de 90 MPa, como era esperado, nas frequencias mais baixas, as taxas de aceleraçao da trinca foram mais elevadas. No entanto, os testes realizados sob pressão de 0.6 MPa apresentaram resultados atipicos, com valores de da/dN inferiores ao esperado para frequências inferiores a 1 Hz, contrariando o senso comum de que baixas frequencias conduzem a altas taxas de propagação, devido ao fenomeno de fragilização por hidrogênio. As superficies de fratura analizadas por microscopia eletronica de varredura indicaram que o numero de facetas frageis e o numero de estriaçoes foram também afetadas pelo hidrogenio.
Palavras-chave: Fragilizaçao por hidrogênio; Propagaçao de trinca; Aço Ni-Cr-Mo.

[1] *Technical contribution to 65th ABM Annual Congress, July, 26th to 30h, 2010, Rio de Janeiro, RJ, Brazil.*
[2] *PhD student, Graduate School of Engineering, Kyushu University, Fukuoka, Japan.*
[3] *Professor Department of Mechanical Engineering Science, Kyushu University / National Institute of Advanced Industrial Science and Technology (AIST), Fukuoka, Japan.*
[4] *Vice-Chancellor and Trustee, Professor Department of Mechanical Engineering Science, Kyushu University, Director of Research Center for Hydrogen Industrial Use and Storage (Hydrogenius), National Institute of Advanced Industrial Science and Technology (AIST), Fukuoka, Japan.*
[5] *Air Liquide R & D, Hydrogen Energy Domain Director, Centre de Recherche Claude-Delorme (CRCD), Les Loges-en-Josas, France.*
[6] *Member of ABM, Air Liquide R & D, International Expert R&D-Physical Metallurgy, CRCD, Les Loges-en-Josas, France / Special Appointment Prof. Dep.of Mechanical Engineering Science, Kyushu University, Fukuoka, Japan.*

ISSN 1516-392X

1 INTRODUCTION

To construct a hydrogen based society, hydrogen energy systems (fuel cell vehicles-FCV, and stationary fuel cells) and hydrogen energy infrastructures (hydrogen filling stations and pipelines) are being developed. Japan is currently conducting the Japan Hydrogen and Fuel Cell Demonstration Project (JHFC), a two phase project scheduled for the period of 2002 - 2010 aiming to demonstrate the technical viability of FCV and high pressure hydrogen filing stations. The phase I of this project has ended in 2005 with demonstrations of 35 MPa FCVs and a 40 MPa hydrogen filling station. The second phase of this project started in 2006, and should finish in 2010, with exhibitions of 70 MPa FCVs and 80 MPa hydrogen filling station. The 70/80 MPa hydrogen pressure energy systems are also being researched in the USA and in Germany.

Based on their hardenability, two steels have be chosen for the stationary storage metallic cylinder (type I) of a hydrogen filling station (HFS): the Cr-Mo (JIS-SCM435) steel is the candidate for a 35 MPa HFS and the Ni-Cr-Mo (JIS-SNCM439) steel is the preferred candidate for 70 MPa HFS.[1] During the operation of a filling station, the hydrogen filling sequence will have an impact on the fatigue and fracture resistance of the steel used for the hydrogen storage cylinder. As an example, in the case of the hydrogen filling operation of a 35 MPa FCV cylinder, firstly the FCV tank will be filled up with hydrogen to 20 MPa, followed by 30 MPa and finally the tank is filled up to 35 MPa of hydrogen pressure. A similar sequence with a maximum hydrogen pressure of 70 MPa is used for the 70 MPa FCV cylinders.

The emptying and filling processes will subject the hydrogen storage cylinder of the filling station to cyclic loads while under hydrogen gas pressure. Therefore, it is necessary to study how different hydrogen pressures and loading frequencies will affect the fatigue properties of the chosen SCM435 and SNCM439 low alloy steels, especially the fatigue crack growth (FCG) rate. In the present work, the fatigue crack growth properties of Ni-Cr-Mo (SNCM439) low alloy steel were studied, and the effect of hydrogen on fatigue fracture modes clarified.

2 MATERIAL AND EXPERIMENTAL PROCEDURES

In this research work, the material used is the Ni-Cr-Mo (JIS-SNCM439) low alloy steel, a candidate material to stationary high pressure cylinder of a hydrogen filling station. Its dimensions are shown in Figure 1; the steel chemical composition is given in Table 1 and its tensile properties in Table 2. Once the tank is formed by forging, it is quenched at 860℃ and tempered at 630℃ (Table 3). Inner and outer areas of the tank walls were analyzed to verify the differences due to the tank fabrication process and the imposed heat treatment. The measurements of the Vickers hardness for the entire thickness of the tank where carried out and reveals a rather uniform hardness distribution with an average of 292 (Figure 2).The tempered martensite microstructure shown in Figures 3 and 4 also reveals no major differences in the inner and outer sections analyzed by optical and with FEG-SEM electron back scattered diffraction (EBSD) microscopy methods. The prototype cylinder complies with the mechanical properties required for stationary hydrogen filling station application, despite the large MnS and Al203 inclusions found in the steel, as shown in Figures 5 and 6.

ISSN 1516-392X

In order to carry out fatigue crack propagation tests, CT specimens were cut out of the bulk of the cylinder prototype and in accordance to the ASTM E647 standard.[2] The CT specimen dimensions and cutting orientations are shown in Figures 7 and 8.

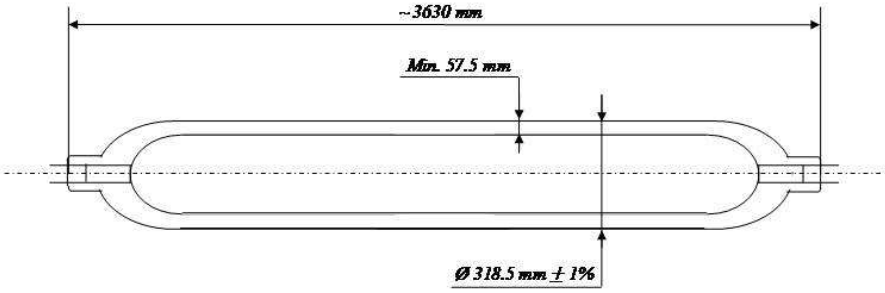

Figure 1. Shape and dimensions of the high pressure hydrogen tank prototype.

Table 1. Chemical composition of SNCM439 steel (wt %)

Element / Symbol	C	Si	Mn	P	S	Ni	Cr	Mo
SO	0.43	0.28	0.82	0.004	0.002	1.95	0.9	0.23
SI	0.43	0.27	0.82	0.005	0.002	1.95	0.91	0.23
SNCM439 Standard value	0.36 ~ 0.43	0.15 ~ 0.35	0.60 ~ 0.90	≤ 0.030	≤ 0.030	1.60 ~ 2.00	0.60 ~ 1.00	0.15 ~ 0.30

Table 2. Mechanical Properties of SNCM439

Yield Stress σ_Y (MPa)	Tensile Strength σ_B (MPa)	Elongation at Fracture δ (%)	Reduction of area ϕ (%)
754	927	17.1	55.3

δ: elongation at fracture; ϕ: reduction of area; $\sigma_B=\sigma_{UTS}$; $\sigma_Y=\sigma_{YS}$

Table 3. Heat treatment of the SNCM439 steel cylinder prototype

	Quenching	Tempering
Hardness	3.30 ~ 3.50 BHD	
Oven	Barell furnace	Barell furnace
Heating temperature	860°C	620°C
Cooling method	Water spray	Air cooling

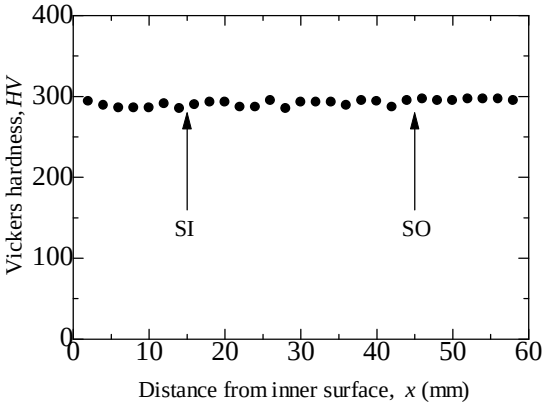

Figure 2. Distribution of Vickers hardness through the thickness in the radial direction from inner to outer surface perpendicular to the loading direction.

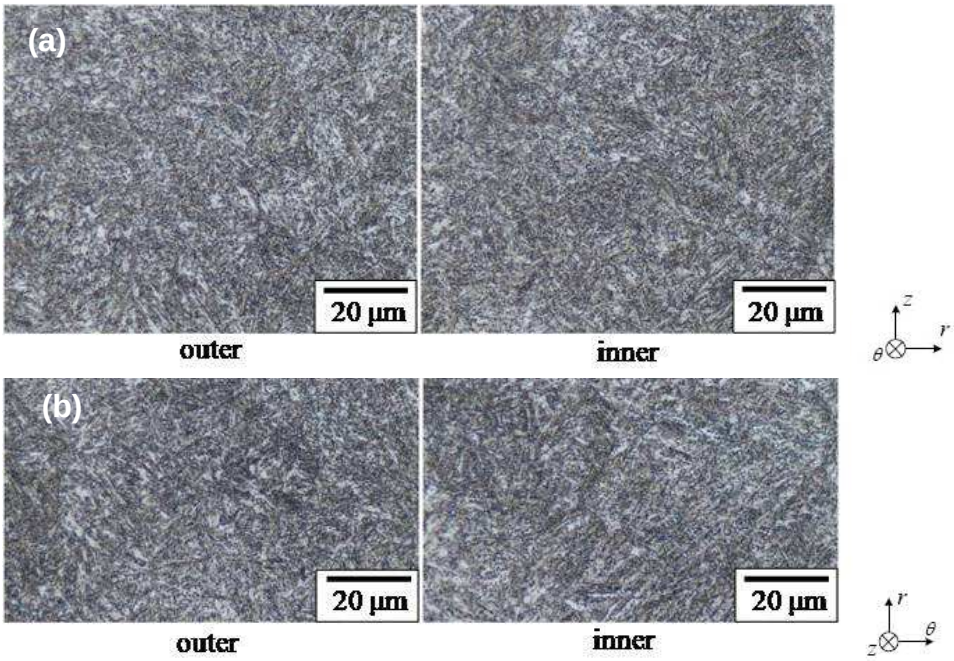

Figure 3. Optical microscopies of the outer and inner sections of SNCM439 steel: a) perpendicular to the circumferential direction, b)Perpendicular to the longitudinal direction.

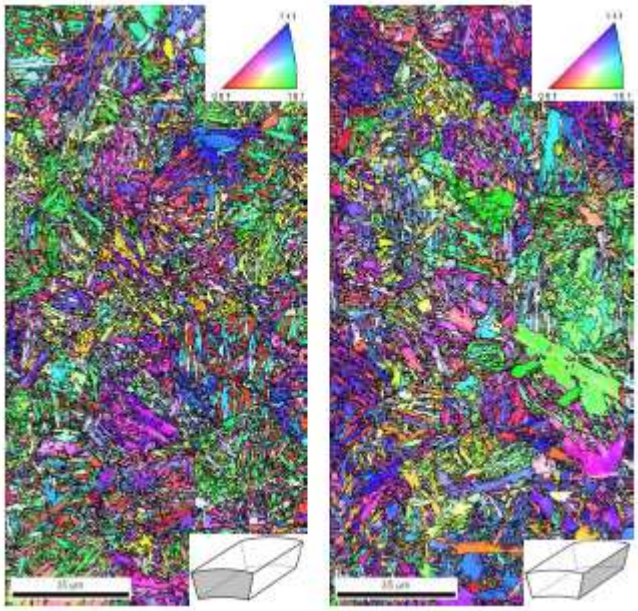

Figure 4. EBSD quality map displaying the crystallographic orientation of the tempered martensite grains of the SNCM439 steel: a) perpendicular to cylinder longitudinal direction, b) perpendicular to cylinder circumferential cross section direction.

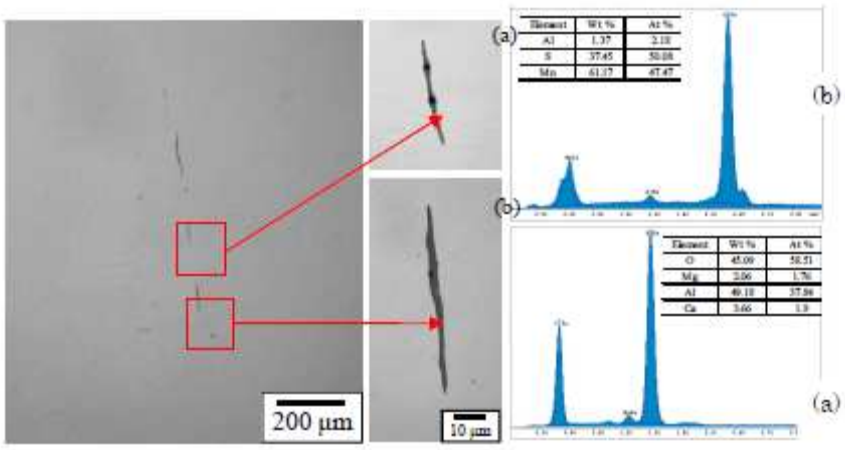

Figure 5. Inclusion observed in a polished surface: (a) Al2O3 inclusions, (b) MnS inclusions.

Figure 6. Inclusions observed on a polished surface of SNCM439 steel.

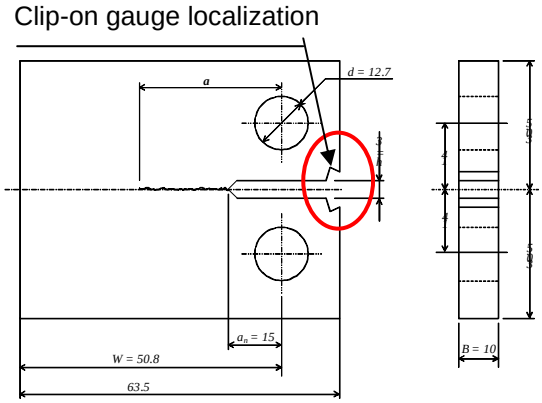

Figure 7. CT specimen details. All dimensions are in mm.

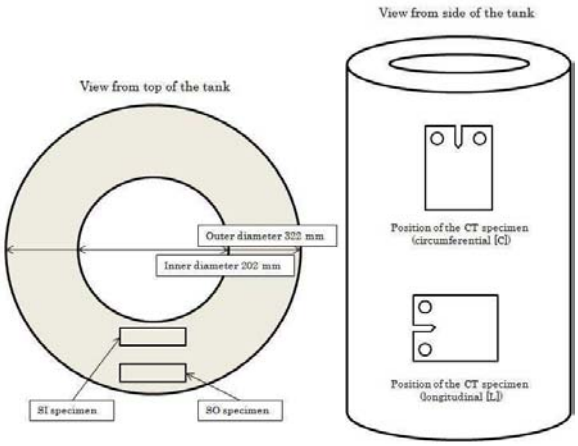

Figure 8. Position of the inner (SI) and outer (SO) CT specimens.

2.1 Experimental Procedure

Regarding to Figure 8, the CT specimens identification is as the following: SCI**, SLI**, SCO**, SLO**, with S: Specimen, C: Circumferential, L: Longitudinal, I: Inner and O: Outer, with ** being the specimen number. Prior to carry out the fatigue crack propagation tests, all specimens were initially pre-cracked in air at room temperature, regardless of the testing environment, with a stress ratio of R = σmin/σmax = 0.1, and at 20 Hz. Then, if the specimen was to be tested in hydrogen, it would also undergoes pre-cracking under the required hydrogen testing pressure, and also with R = 0.1.

The fatigue crack growth tests were conducted in air or hydrogen at room temperature. The stress ratio for all fatigue crack propagation tests was R = 0.5. In hydrogen environment, the hydrogen gas pressures used were: 0.6, 10, 40, 45 and 90 MPa. The selected test frequencies were: 0.01, 0.1, 1, 5 and 20 Hz. Three types of fatigue crack propagation tests have been employed, namely: ΔK-constant with different pressures and frequencies, ΔK-increasing, and ΔK-decreasing. The fatigue servo-hydraulic testing machine was controlled by an automatic feedback control loop that was adjusted by the instantaneous measurements of the crack length using the compliance method with a clip-on gauge, mounted in the open mouth of the CT specimen as indicated n Figure 7.

Prior to any metallographic and microscopy observation, specimens were cut with an A100N type disk and cleaned with acetone. The SEM observations were made at an intensity of 10.0 μA and a voltage of 10.0 ~ 15.0 kV, with a high resolution focus mode. The working distance was 20 ~ 22.6 mm. The EBSD observations required a more dedicated metallographic preparation in order to remove any strain hardening due to mechanical polishing. Details of the EBSD preparation are given elsewhere.[3]

3 EXPERIMENTAL RESULTS AND DISCUSSION

3.1 Fatigue Crack Growth Rates

The data for the crack growth rate plotted against the stress intensity factor range for a frequency of f = 1 Hz in hydrogen gas is represented in Figure 9. The effect of hydrogen on the crack growth rate is dependent on the stress intensity factor range, with an actual acceleration of the crack growth rate in hydrogen for ΔK ≥ 7 Mpa.m1/2 in 90 Mpa and 0.6 Mpa hydrogen gas. The acceleration of da/dN was greater in 90 Mpa than in 0.6 Mpa. In order to verify the effect of hydrogen pressure and testing frequency on the fatigue crack propagation rate of SNCM439 steel, the ΔK-constant test has been used, and a crack growth acceleration rate defined by the relationship between crack propagation rate in hydrogen and the crack propagation rate in air ((da/dN)H2/(da/dN)air) at ΔK = 17.5 Mpa.m1/2 and f = 1 Hz (Figures 9-11).

The crack growth acceleration rate increases linearly with the increase of hydrogen pressure, until it reaches an upper limit of 86 times faster than in air at 90 Mpa at frequencies lower or equal to 0.1 Hz. In the case of lower hydrogen pressures, 0.6 Mpa for example, this upper limit is about 5.6 times faster at 1 Hz, as shown in Figure 11. The crack growth rate acceleration will actually decrease for testing frequencies lower than 1 Hz in 0.6 Mpa hydrogen gas, whether the CT specimen orientation is longitudinal or circumferential. This result is rather surprising and it is against the common knowledge that lower testing frequencies lead to higher fatigue crack growth (FCG) rates.[4-6] It is argued that in the case of this low pressure

hydrogen gas (0.6 Mpa) as well as low frequency (0.1 ~ 0.01 Hz), hydrogen may have enough time to diffuse away from the crack tip plastic zone, thus lessening its embrittlement effect within the process zone immediately ahead of the crack tip. Beachem[7] explains that hydrogen seeks zones of high triaxial stresses and is also trapped by deformations which could explain why in this case hydrogen affects not only the plastic zone ahead the crack tip, but rather it affects also regions that are away from the crack tip. This finding needs to be further investigated.

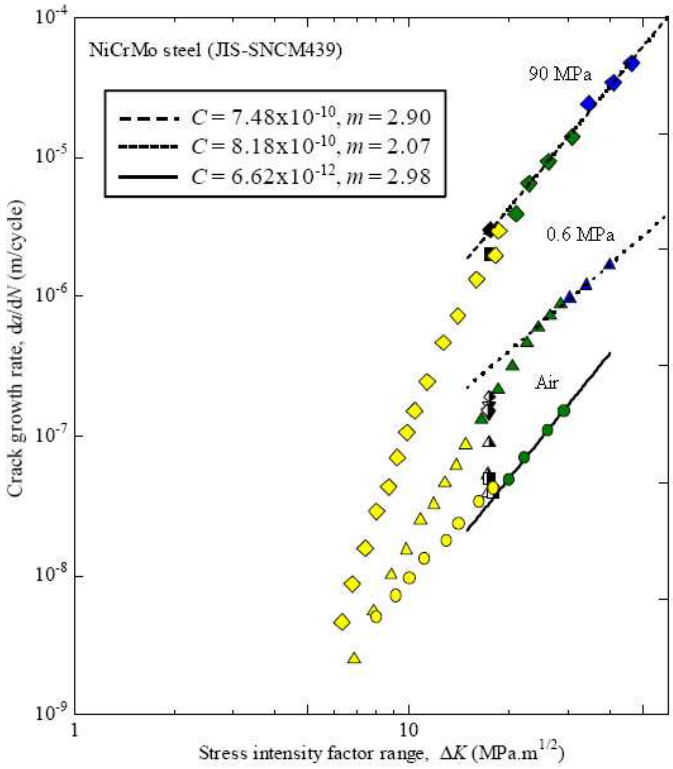

Symbol	Env. (MPa)	Frequency f (Hz)	Test type	Specimen type
◆	H_2, 90	1	ΔK increasing	SCI
◆	H_2, 90	1	ΔK increasing	SCO
◇	H_2, 90	1	ΔK decreasing	SCO
▲	H_2, 0.6	1	ΔK increasing	SLI
▲	H_2, 0.6	1	ΔK increasing	SCI
△	H_2, 0.6	1	ΔK decreasing	SCI
●	Air	20	ΔK increasing	SCI
○	Air	20	ΔK decreasing	SCI
■	H_2, 90	0.01	ΔK constant	SCI
▲	H_2, 90	0.1	ΔK constant	SCI
◆	H_2, 90	1	ΔK constant	SCI
◨	H_2, 0.6	0.01	ΔK constant	SCI
◭	H_2, 0.6	0.1	ΔK constant	SCI
◆	H_2, 0.6	1	ΔK constant	SCI
▽	H_2, 0.6	5	ΔK constant	SCI

Figure 9. Crack growth rate da/dN vs. stress intensity factor range ΔK in air and in hydrogen.

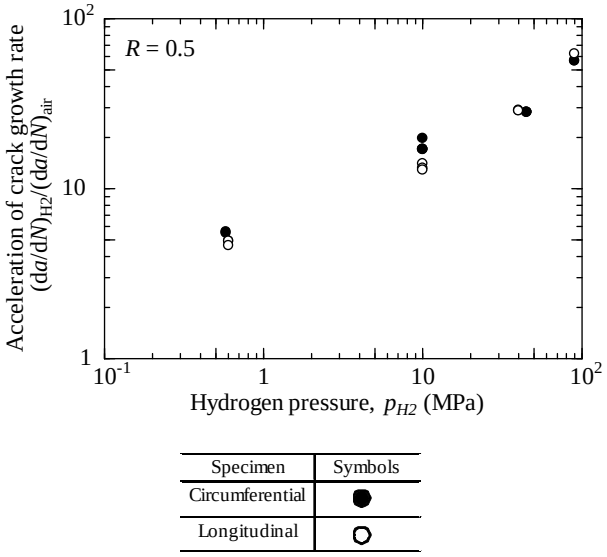

Figure 10. Acceleration of crack growth rate $(da/dN)_{H2}/(da/dN)_{air}$ vs. hydrogen pressure (p_{H2}) for the circumferential and longitudinal specimens at ΔK=17.5 MPa.m$^{1/2}$

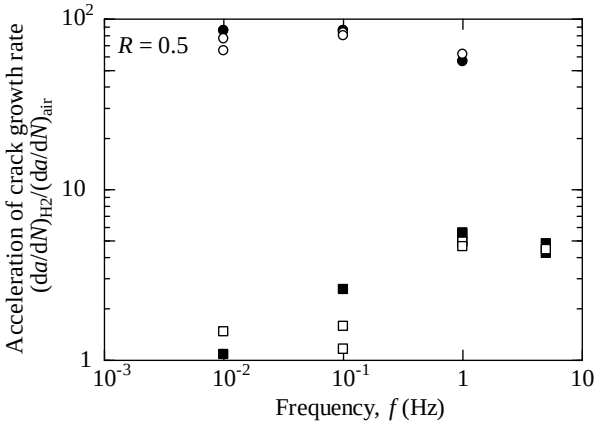

Figure 11. Acceleration of crack growth rate $(da/dN)_{H2}/(da/dN)_{air}$, vs. frequency f for circumferential and longitudinal specimens at ΔK=17.5 MPa.m$^{1/2}$

3.2 Fracture Surfaces

By observing the fracture surfaces of tested CT samples with SEM it was possible to identify and measure manganese sulfide (MnS) and alumina (Al2O3) inclusions (Figure 12). Visible parts of elongated MnS inclusions were found on the fracture surface measuring up to 307 μm in length and up to 5 μm in diameter, and up to 4 μm in diameter for Al2O3 inclusions. Yano et al.[8] have carried out a detailed analysis of the inclusions found in the same steel and observed that alumina inclusions were reportedly more numerous, and assembled in clusters. In the present study, for the CT specimens taken in the C-direction, the manganese sulfide inclusions are in the same direction of the crack propagation, while they are perpendicular to the crack path in the L-direction CT specimens, due to the manufacturing process. Thornton[9] has called attention about the inclusions orientation and their effect on fatigue resistance. He has pointed out that inclusions with their long axis normal to the principal tensile stress direction are very likely to initiate fatigue failure. However the effects of inclusions on the FCG rate seem to be less obvious. According to our results presented in Figure 9 and the observation of inclusions on the fracture surface, even for the more critical orientation of the CT specimen, e.g., the circumferential direction, MnS (Figure 12) inclusions did not affect the fatigue crack growth rate of SNCM439 steel.

On the contrary, Yano et al.[8] have found that fatigue crack initiation is largely dependent upon the existence of surface or subsurface defects, such as inclusions. They reported that in the case of smooth and round specimens inclusions indeed decreased the fatigue life of SNCM439 low alloy steel samples as they shorten the initiation period of the fatigue life.

ISSN 1516-392X

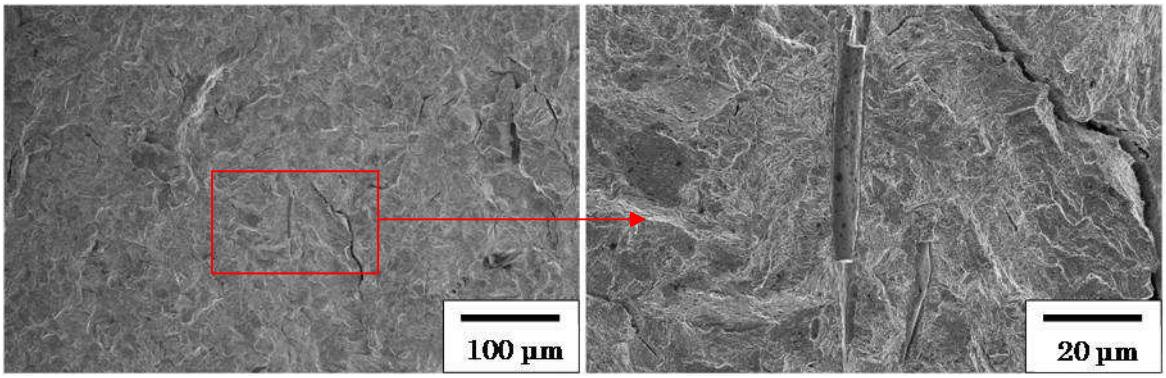

Low magnification High magnification

Figure 12. MnS inclusion on the fracture surface of a C-direction specimen (SEM) in 90 MPa hydrogen at 1 Hz, ΔK = 17.5 Mpa.m1/2

Regarding to the effect of hydrogen on FCG rates the fracture surfaces analyzed reveal the presence of facets, smooth areas, like the ones presented in Figure 13, placed perpendicularly to the applied load. They appeared regardless the hydrogen pressure used in the fatigue test. They could be regarded as a footprint of the effect of hydrogen in accelerating the crack propagation rate. Those facets are completely absent of the fracture surfaces of the specimen tested in air, which is dominated by the presence of fatigue striations as observed in Figure 13.

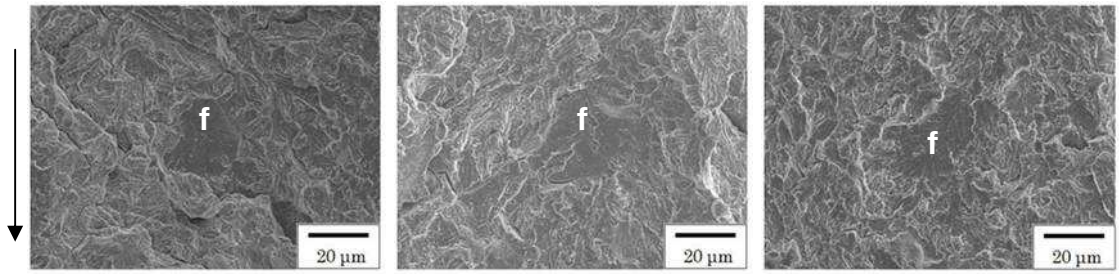

(a) Under 90 MPa, at 0.01 Hz (b) Under 45 MPa, at 1 Hz (c) Under 10 MPa, at 1 Hz

Figure 13. Facets (f) in SNCM439 steel tested in hydrogen at various pressures and under ΔK-constant, ΔK = 17.5 MPa.m1/2. The arrow indicates the crack propagation direction.

The distribution of facets on crack surface and their correlation to □□ values is shown in Figure 14. The number of facets is directly linked to hydrogen pressure; however it seems to have little influence on the fatigue crack growth rate.

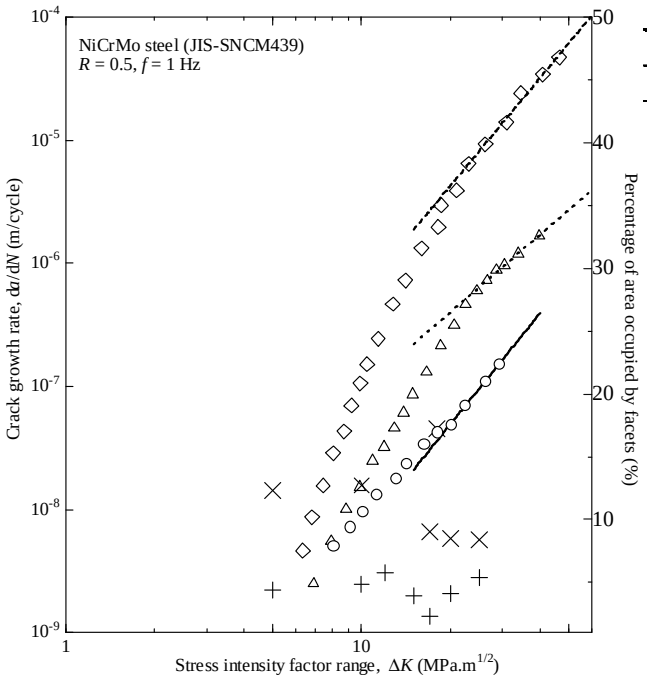

Environment	Symbol for facets
0.6 MPa hydrogen	+
90 MPa hydrogen	×

Environment	Frequency (Hz)	
	1	20
90 MPa hydrogen	◇	-
0.6 MPa hydrogen	△	-
Air	-	○

Figure 14. Percentage of surface occupied by facets vs. stress intensity factor range, comparison with the crack growth rate.

SEM observations of fracture surfaces also showed that the striation fracture mode is also affected by hydrogen when compared to striations found in samples tested in laboratory air. The striation spacing becomes wider when the specimens were tested in hydrogen gas, with an average striation spacing of 0.183 μm in 0.6 Mpa hydrogen gas and around 0.276 μm in 90 Mpa hydrogen gas. For comparison, the average striation spacing in air is around 0.183 μm (Figure 15).

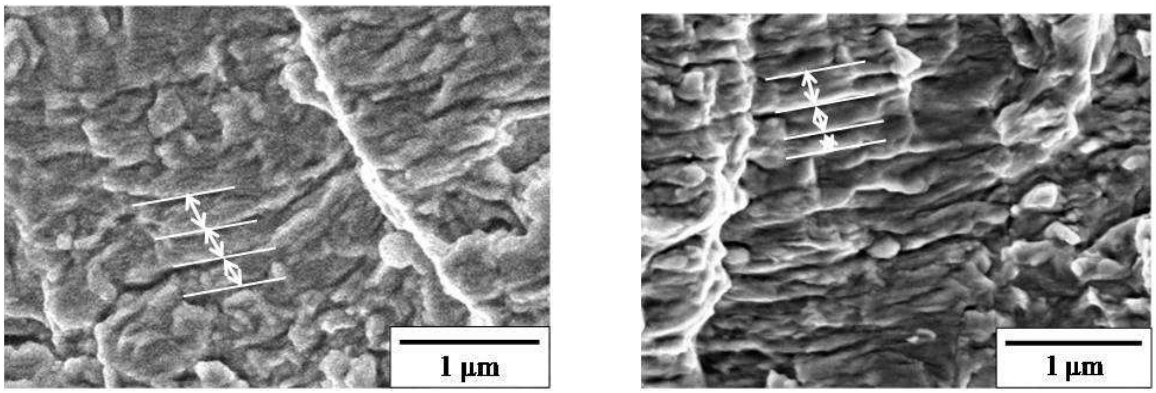

(a) In air (b) In 0.6 Mpa hydrogen gas

Figure 15. Striations in air and hydrogen gas at ΔK =17.5 MPa.m1/2

3.3 Slip Bands and Cracks

The observation of slip bands on polished surfaces of CT specimens were carried out with the aid of a laser microscope. Figures 16 - 19 show the crack path and the slip band pattern of specimens tested in air and in various hydrogen gas pressures at different frequencies, but at a constant ΔK = 17.5 MPa.m1/2. The specimen surface in hydrogen is smoother when compared to the specimen tested in air, i.e., slip bands are less visible on the specimen tested in hydrogen. This is a clear indication of the effect of hydrogen on the acceleration of fatigue crack propagation rate as the

slip bands at the crack tip tend to be more localized at the crack tip due to the diffusion of hydrogen to this area.

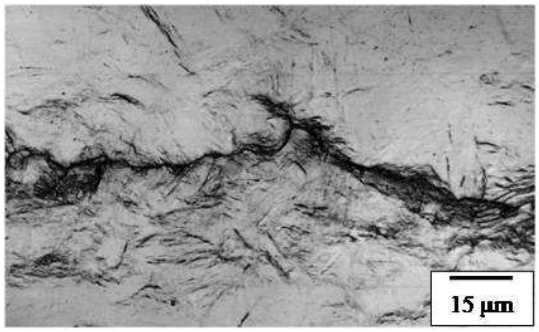

Figure 16. Crack in air, at 20 Hz, ΔK = 17,5 MPa.m$^{1/2}$

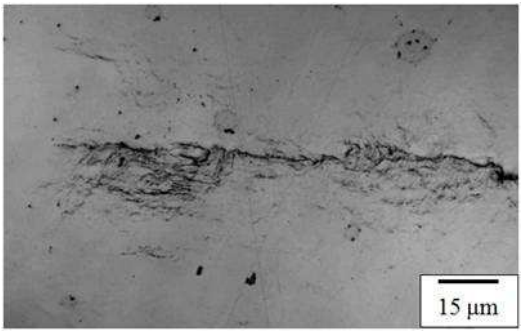

Figure 17. Crack tip in 0.6 MPa H_2 gas, at 0.01 Hz, ΔK = 17,5 MPa.m$^{1/2}$

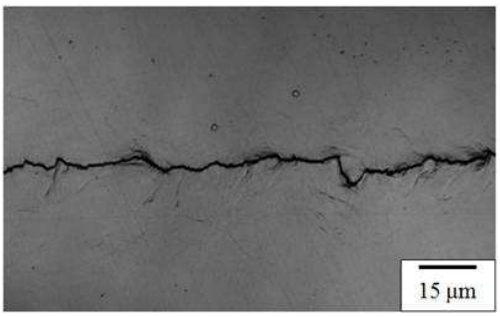

Figure 18. Localized slip in 45 MPa hydrogen gas, at 1 Hz, ΔK = 17,5 MPa.m$^{1/2}$

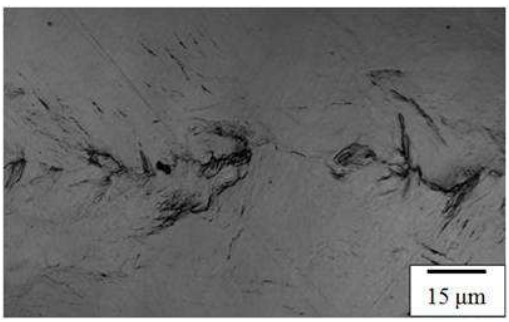

Figure 19. Localized slip in 10 MPa hydrogen gas, at 1 Hz, ΔK = 17,5 MPa.m$^{1/2}$

4 CONCLUSIONS

It was investigated the effect of hydrogen pressure and loading frequency on the FCG rates of SNCM439 steel, a candidate to stationary storage cylinder of hydrogen filling stations. The obtained results may be summarized as the following:

It has been shown that loading frequency affects the crack growth rate in hydrogen. At 90 MPa of hydrogen pressure, the crack growth rate rises as the frequency decreases, until 0.1 Hz. After this value, decreasing frequency does not seem to accelerate further the crack growth. The comparison between fatigue tests in air and fatigue tests in hydrogen shows that the crack growth rate can be accelerated up to 86 times, at a ΔK=17.5 MPa.m1/2, and with the lowest frequency (0.1 Hz or 0.01 Hz) and the highest pressure tested (90 MPa).

Specimens tested in hydrogen environment have a higher crack growth rate than specimens tested in air, with higher hydrogen pressures resulting in higher crack growth rates. At ΔK=17.5 MPa.m1/2, the acceleration of crack growth rate (da/dN)H2/(da/dN)air increases linearly on a log-log scale with hydrogen pressure.

The results obtained in low-pressure hydrogen environment (0.6 MPa) are rather surprising. Contrary to the common belief that lowering the test frequency the higher will be FCG rates. Considering the constant ΔK= 17.5 MPa.m1/2, the acceleration of crack growth rate was around 5.6 at 1 Hz, while the acceleration rates at 0.1 Hz and 0.01 Hz were 2.6 and 1.1, respectively. However, these findings need to be further investigated.

It has been also found that MnS inclusions orientation, whether the inclusions were parallel or orthogonal to crack growth direction, has little effect on fatigue crack growth in hydrogen environment, when comparing test results in air and in hydrogen gas. And finally, it is pointed out that the orientation of CT specimens in relation to the loading direction doesn't seem to have a significant influence on the experimental results.

Acknowledgements

This research was supported by the NEDO Fundamental Research Project on Advanced Hydrogen Science (2006 to 2012).

REFERENCES

1 Japan Hydrogen & Fuel Cell Demonstration Project, http://www.jhfc.jp
2 ASTM E 647 – 05: Standard Test Method for Measurement of Fatigue Crack Growth Rates, ASTM INTERNATIONAL 2005:45.
3 MINE, Y.; HORITA, Z.; and MURAKAMI, Y. Effect of hydrogen on martensite formation in austenitic stainless steels in high-pressure torsion, Acta Materialia 57 (2009) 2993–3002.
4 TOPLOSKY, J.; RITCHIE, R.O. On the Influence of Gaseous Hydrogen in Decelerating Fatigue Crack Growth Rates in Ultrahigh Strength Steels, Scripta Metallurgica, Vol. 15, 1981, pp. 905-908
5 MUSUVA, J.K.; RADON, J.C. The Effect of Stress Ratio and Frequency on Fatigue Crack Growth, Fatigue of Engineering Materials and Structures Vol. 1, 1979, pp 457-470.
6 CLARK, W.G.; LANDES, J.D. An Evaluation of Rising Load KIscc Testing, Stress Corrosion - New Approaches, ASTM STP 610, 1976, pp. 108-127.
7 BEACHEM, C.D. A New Model for Hydrogen-Assisted Cracking (Hydrogen "Embrittlement"), Metallurgical Transactions, Vol. 3, Feb. 1972 – 437
8 YANO, H.; HOMMA, N.; FUKUSHIMA, Y.; MACADRE, A.; FURTADO, J.; MATSUOKA,S. Effects of Hydrogen and Testing Frequency on Fatigue Properties of JIS-SNCM439 for Storage Cylinder of 70 MPa Hydrogen Station, submitted to the Trans. Japanese Society of Mechanical Engineering A.
9 THORNTON, P.A. The Influence of Nonmetallic Inclusions on the Mechanical Properties of Steel: A Review, Journal of Materials Science 6, 1971, 347-356.